Sculpting Liquids with Two-Dimensional Materials: The Assembly of Ti$_3$C$_2$T$_X$ MXene Sheets at Liquid−Liquid Interfaces

Jeffrey D. Cain,[‡,§] Amin Azizi,[†,§] Kathleen Maleski,[∥,⊥] Babak Anasori,[∥,⊥,○] Emily C. Glazer,[†,‡,§] Paul Y. Kim,[‡] Yury Gogotsi,[∥,⊥] Brett A. Helms,[‡,#] Thomas P. Russell,[‡,¶,□] and Alex Zettl[*,†,‡,§]

[†]Department of Physics, University of California at Berkeley, Berkeley, California 94720, United States

[‡]Materials Sciences Division, Lawrence Berkeley National Laboratory, Berkeley, California 94720, United States

[§]Kavli Energy NanoSciences Institute at the University of California at Berkeley and the Lawrence Berkeley National Laboratory, Berkeley, California 94720, United States

[∥]Department of Materials Science & Engineering, Drexel University, Philadelphia, Pennsylvania 19104, United States

[⊥]A.J. Drexel Nanomaterials Institute, Drexel University, Philadelphia, Pennsylvania 19104, United States

[#]The Molecular Foundry, Lawrence Berkeley National Laboratory, Berkeley, California 94720, United States

[¶]Department of Polymer Science and Engineering, University of Massachusetts Amherst, Amherst, Massachusetts 01003, United States

[□]Beijing Advanced Innovation Center for Soft Matter Science and Engineering, Beijing University of Chemical Technology, Beijing 100029, China

[○]Integrated Nanosystems Development Institute, Department of Mechanical and Energy Engineering, Purdue School of Engineering and Technology, Indiana University−Purdue University Indianapolis, Indianapolis, Indiana 46202, United States

ABSTRACT: The self-assembly of nanoscale materials at the liquid−liquid interface allows for fabrication of three- dimensionally structured liquids with nearly arbitrary geometries and tailored electronic, optical, and magnetic properties. Two-dimensional (2D) materials are highly anisotropic, with thicknesses on the order of a nanometer and lateral dimensions upward of hundreds of nanometers to micrometers. Controlling the assembly of these materials has direct implications for their properties and performance. We here describe the interfacial assembly and jamming of Ti$_3$C$_2$T$_x$ MXene nanosheets at the oil−water interface. Planar, as well as complex, programmed three- dimensional all-liquid objects are realized. Our approach presents potential for the creation of all-liquid 3D-printed devices for possible applications in all-liquid electrochemical and energy storage devices and electrically active, all-liquid fluidics that exploits the versatile structure, functionality, and reconfigurability of liquids.

KEYWORDS: *2D materials, MXenes, liquid−liquid interfaces, self-assembly, structured liquids*

2D MXene Assembly → 3D Sculpted Liquids
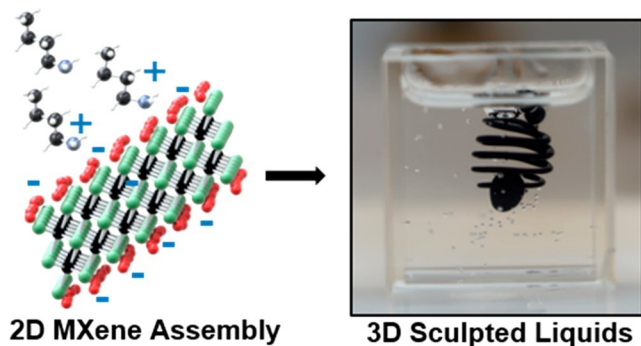
MXenes represent a growing family of two-dimen- sional (2D) transition metal carbides, nitrides, and carbonitrides derived from three-dimensionally bonded MAX phases or other layered precursors.[1] The MAX phases, one precursor used to synthesize the MXenes, take their name from their composition; specifically, $M_{n+1}AX_n$ ($n = 1$, 2, or 3), where M is an early transition metal (*e.g.*, Ti, V, Nb, Mo), A is a member of group 13 or 14 (*e.g.*, Al, Si), and X is C and/or N. In the bulk, MAX phases are composed of $M_{n+1}X_n$

layers, separated by planes of "A" atoms.[2,3] Since mechanical exfoliation of these materials is extremely difficult, 2D MXenes are historically generated by selectively etching out the "A" planes, typically with an aqueous fluoride-containing acid, followed by an intercalation and exfoliation step, leaving
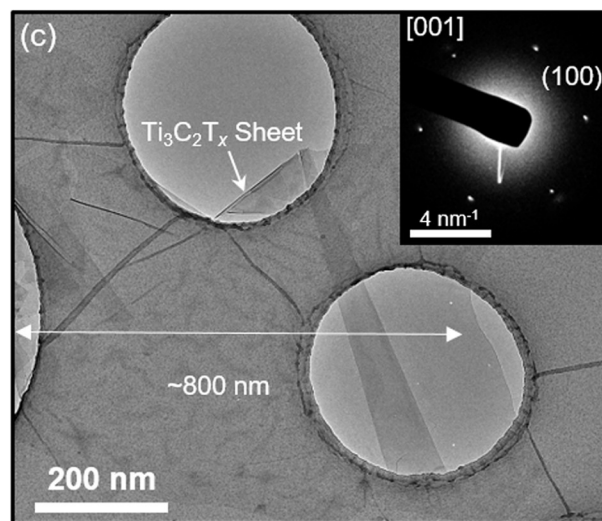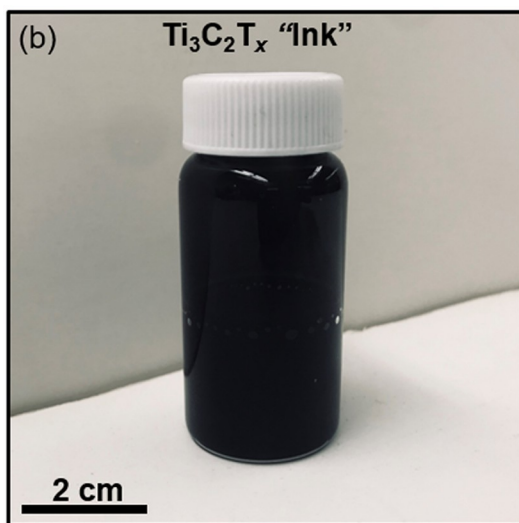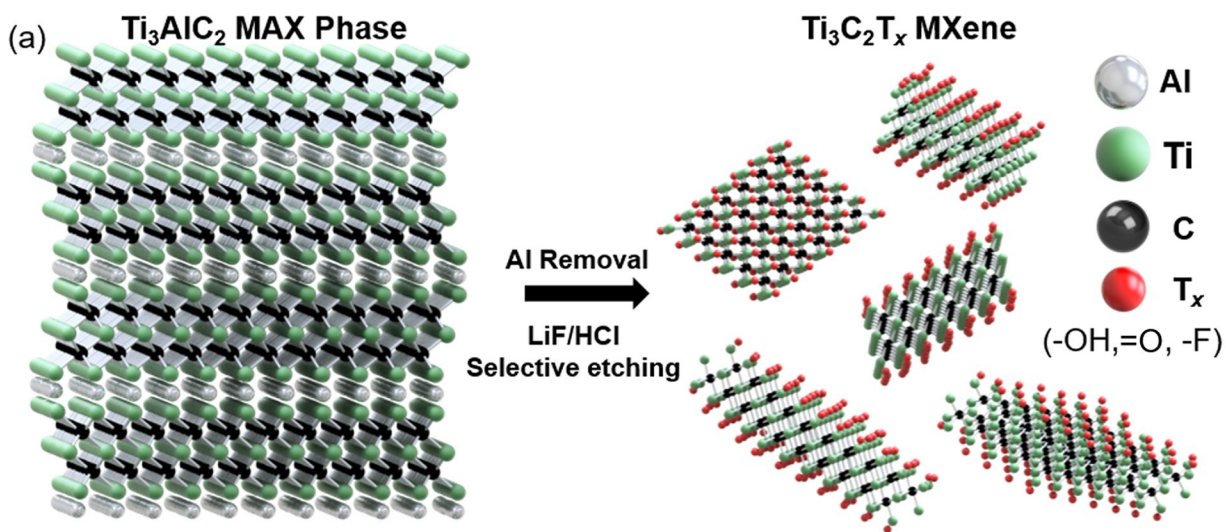
Figure 1. (a) Schematic of the synthesis approach used to transform bulk MAX phase Ti$_3$AlC$_2$ (left) to two-dimensional (2D) Ti$_3$C$_2$T$_x$ MXene sheets. (b) Digital image of 20 mL of the Ti$_3$C$_2$T$_x$ sheets suspended in water (MXene "ink") used for assembly and printing. (c) Transmission electron microscopy image of 2D Ti$_3$C$_2$T$_x$ and its electron diffraction pattern (inset).

behind single layers of M$_{n+1}$X$_n$ (i.e., Ti$_3$C$_2$, Ti$_3$CN) with a thickness of approximately 1 nm.[4–6] As a result of the chemical etching process, the 2D layers are terminated with −OH, =O, and −F functional groups,[7] making them hydrophilic and readily dispersible in water. The synthesis process is shown schematically in Figure 1a. As such, the composition is denoted by M$_{n+1}$X$_n$T$_x$, where T$_x$ represents the possible surface groups. Surface functionalization imbues the sheets with a negative charge, with zeta potentials ranging from −30 to −80 mV, depending on composition.[8] Rheology studies confirmed that Ti$_3$C$_2$T$_x$ dispersions in water[9] and organic solvents[10] exhibit non-Newtonian characteristics and shear thinning behavior, making them capable of ink jet and extrusion printing processes.[11,12] Further, the integration of 2D materials into traditional printing schemes has been heavily investigated.[13,14] MXenes are also characterized by high electrical[15,16] and thermal conductivity,[17] and they have been investigated for use in a wide variety of applications including energy storage technologies,[18–20] water purification and desalination,[21] and conductive coatings for electromagnetic interference shielding and wireless communication.[22,23]

Their versatile properties, two-dimensional nature, inherent surface functionalization/negative charge, and solution proc- essability make MXenes ideal candidates for interfacial assembly and incorporation into structured liquids. The interface between immiscible liquids presents a versatile landscape for the assembly of functional nanomaterials,[24] which can be used to prepare films[25] and emulsions.[26,27] Nanoparticle (or for MXenes, nanosheet) surfactant assemblies have become a ubiquitous process for the preparation of nanomaterials and have been demonstrated with graphene oxide (GO),[28] carbon nanotubes (CNTs),[29] and metallic/ semiconducting nanoparticles, among other materials.[30]

Nanoparticle surfactant film assemblies can be used to impart structure and mechanical stability to liquid−liquid interfaces *via* jamming. Functionalized nanomaterials can self-

assemble and form a monolayer of nanoparticle surfactants at the interface and thereby reduce the interfacial tension. Under external perturbation (*e.g.*, electrical field, mechanical deforma- tion), the interface can deform and the interfacial area will increase, which allows additional nanoparticle surfactants to assemble at the newly formed interface. Upon removal of the
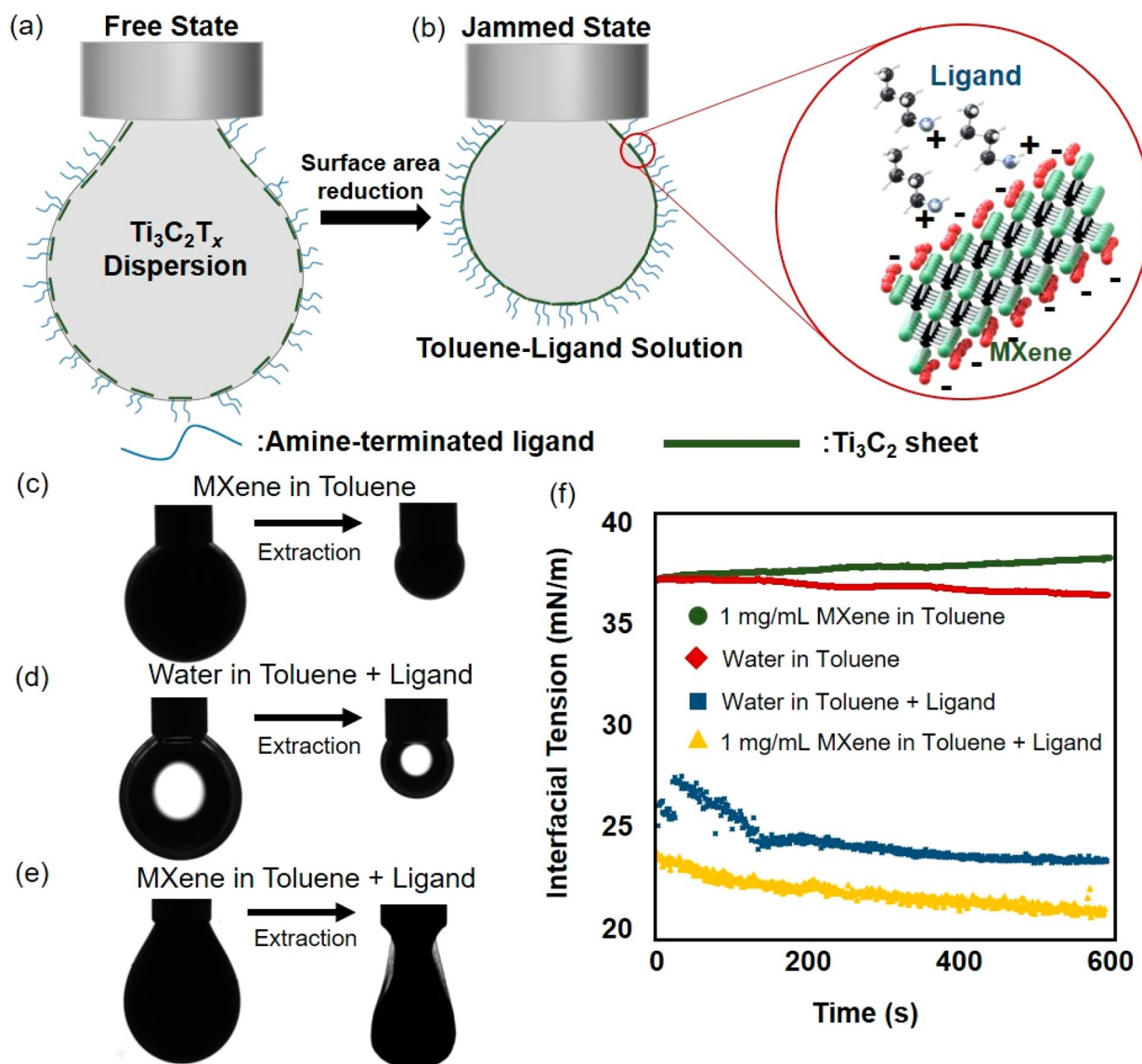
Figure 2. Schematic of pendant drop tensiometry in (a) the free state and formation of (b) the jammed state upon extraction and a schematic of the assembly of $Ti_3C_2T_x$ MXene sheets with *n*-butylamine. Optical images of pendant drop specimens before and after extraction of (c) $Ti_3C_2T_x$ in toluene without ligands, (d) water in toluene with *n*-butylamine ligands, and (e) $Ti_3C_2T_x$ in toluene with ligands showing relaxation of the drop and buckling of the jammed film upon extraction. (f) Interfacial tension as a function of time for water and $Ti_3C_2T_x$ ink against toluene with and without ligands.

perturbation, the interface attempts to relax and minimize the surface area, but is impeded by the nanoparticle surfactants jammed at the interface. The jamming process has been used for the creation of nonequilibrium shapes,[31] bicontinuous jammed emulsions (bijels),[32] and three-dimensionally struc- tured liquids with arbitrary geometries.[33] Structured liquids of this type have been considered for applications in all-liquid reaction vessels, energy storage materials, and fluidic devices.[34] Here, we report on the interfacial assembly of 2D $Ti_3C_2T_x$ MXene nanosheets at oil−water interfaces and the formation of structured liquids stabilized by the 2D nanosurfactants jammed at these interfaces. We take advantage of the inherent surface functionalization and negative charge that arises from the chemical processes used for dimensional reduction from 3D MAX phases to 2D MXenes. We enhance the interfacial activity of the $Ti_3C_2T_x$ *via* ligands in the opposite phase with appropriate chemistry/charge. The $Ti_3C_2T_x$ nanosheets

interact with ligands with a complementary termination at the interface, forming nanosheet surfactants and binding them to the interface. The formation, assembly, and jamming of the MXene nanosheet surfactants is taken advantage of for the preparation of planar MXene films and the three-dimensional sculpting of biphasic liquid mixtures. Further, we show that 3D printing can be used to sculpt the interfacial constructs into arbitrary, three-dimensional, nonequilibrium geometries.

RESULTS AND DISCUSSION

Two-dimensional $Ti_3C_2T_x$ MXene sheets were prepared using standard chemical etching techniques reported elsewhere (and detailed in the Experimental Section).[16] Briefly, $Ti_3C_2T_x$ was obtained from Ti_3AlC_2 MAX phase precursor. Ti_3AlC_2 powder was added to LiF and HCl and allowed to react, resulting in the removal of Al from the 3D Ti_3AlC_2 MAX phase, as shown schematically in Figure 1a. Further processing was done to

separate single- and few-layer $Ti_3C_2T_x$ from multilayer MXene and unreacted MAX phase. The result was a black, viscous, ink- like dispersion with a concentration range of 10−15 mg mL^{-1}
(as characterized by UV−vis spectroscopy, Figure S1).
Importantly, this process imbues the MXenes sheets with the
negative surface charge necessary for the assembly described below. Deaerated water is used to minimize degradation of the MXenes in aqueous media during storage; additionally, the dispersion is stored in argon-sealed vials and refrigerated.

For assembly experiments, the dispersion is retrieved from argon-sealed vials and diluted with deionized (DI) water to a desired concentration (1−7.5 mg mL^{-1}), resulting in MXene
"inks", shown in Figure 1b. Diluted dispersions are used within
hours to avoid any potential degradation of the material. The resulting $Ti_3C_2T_x$ flakes are imaged using transmission electron microscopy (TEM) to deduce lateral dimensions and confirm crystallinity. As shown in Figure 1c, few-layer sheets exhibit lateral dimensions of hundreds of nanometers (approaching 1 μm), and selected area electron diffraction (Figure 1c, inset) shows the expected hexagonal crystalline symmetry, confirming that the $Ti_3C_2T_x$ is not degraded or oxidized during storage or following dilution with DI water. Dynamic light scattering also confirms lateral dimensions of MXene sheets within the dispersions (Figure S2). For the oil phase, amine-terminated
ligands and multiple hydrophobic solvents are demonstrated for assembly and 3D printing. In a typical experiment, 1−7 wt
% of the ligand is dissolved/dispersed into toluene or, for 3D
printing experiments, high-viscosity silicone oil. In this work, assembly is demonstrated with the short-chain organic molecule n-butylamine $(CH_3(CH_2)_3NH_2)$. The choice of amine-terminated ligands is motivated by the negative charge naturally present on the $Ti_3C_2T_x$ surface; the amine termination acquires a complementary positive charge on contact with the aqueous phase. This provides an electrostatic attraction between the two components, which drives them to the interface.

The interfacial activity and assembly of the $Ti_3C_2T_x$ at water−oil interfaces were first investigated using pendant drop tensiometry, which monitors the interfacial surface tension as a function of time, as well as the observation of jamming and
wrinkle formation upon surface area reduction by extraction of the MXene phase. This phenomenon is shown schematically in Figure 2a and b; upon injection of the MXene ink into the oil−
ligand solution phase (in this case toluene with n-butylamine),

the MXene sheets diffuse to the interface, forming MXene surfactants with the n-butylamine (see Figure 2b). The MXene surfactants cover the interface (free state), and upon reduction of the interfacial area via extraction of the MXene dispersion
from the droplet, the jammed state is reached. Figure 2c−e
present optical images of this phenomenon, along with control
experiments. In Figure 2c, the MXene dispersion is injected into toluene without ligands and aged for 10 min; upon extraction, no film is formed, meaning the interfacial activity of the MXene on its own is low or nonexistent, due to the
inherent negative charge of the water/toluene interface. Similar results are shown for water injected into the toluene−ligand solution (Figure 2d), where no buckling is present upon extraction, since the compressive force is sufficient to eject individual ligands from the interface. It is best to note that the white "spot" in the pendant drop image is light reflected from
the toluene/ligand solution droplet. In Figure 2e, the MXene solution is injected into the toluene/ligand solution (left) and allowed to age for 10 min. The solution is then quickly (1000

μL/min) extracted, and the MXene surfactants at the interface transition to the jammed state.

Due to the high optical contrast of the MXene dispersion, it is difficult to observe the characteristic buckling at the interface; however, wrinkling can be seen when a significant amount of the MXene dispersion is removed and a film is clearly observed. The interfacial surface tension is also monitored after injection and throughout the aging period and can be seen in Figure 2f. At an MXene concentration of 1 mg mL^{-1} and without ligands in the surrounding oil phase the interfacial surface tension is ~36 mN m^{-1}, equal to that of pure water in toluene.[35] It should be noted that, at long aging times (~1 h and thereafter), or with agitation, some MXene will adsorb to the interface and wrinkling can be achieved (Figure S3), indicative of small interfacial activity of the Ti$_3$C$_2$T$_x$ sheets without the inclusion of complementary ligands in the oil phase. This observation is consistent with a previous report from Dong et al.[36] and others.[37] The adsorption of the MXene sheets without the ligand appears to be a slow process (on the order of 1 h), limited by the diffusion of the sheets to the interface and the electrostatic interaction therein. As shown in Figure 2f, when n-butylamine is added to the oil phase, the interfacial surface tension is reduced to an equilibrium value of 22 mN m^{-1}. The ligands themselves serve to reduce interfacial tension, but do not form interfacial jammed films (Figure 2d), and the inclusion of the Ti$_3$C$_2$T$_x$ reduced the interfacial tension below that of the ligands alone. This confirms that the Ti$_3$C$_2$T$_x$ sheets have interacted with the n-butylamine at the oil−water interface and formed MXene surfactants, reducing the interfacial energy of the two-phase system. This result, combined with the presence of wrinkling of the interface upon extraction, conclusively demonstrates the formation of MXene surfactants and their self-assembly at the oil−water interface. It is instructive to probe the microstructure and morphology of the assembled Ti$_3$C$_2$T$_x$ surfactant film. Figure 3a and b show TEM and optical images of films prepared at a planar interface between an oil−ligand solution and the MXene dispersion. In the TEM image, it can be observed that the assembled film consists of overlapping Ti$_3$C$_2$T$_x$ sheets, rather than a single layer of "tessellated nanotiles" found in graphene oxide assembled at oil−water interfaces.[28] The top inset shows a low-magnification image, demonstrating the continuous nature of the film at micrometer scales. The bottom inset of Figure 3a shows the electron diffraction pattern of the assembled film. The electron diffraction pattern exhibits the polycrystalline rings associated with a randomly oriented film and,

importantly, shows that no structural changes have occurred within the MXene sheets after interaction with the n- butylamine ligands. As noted, the assemblies can be prepared at planar oil−water interfaces (e.g., within a Langmuir trough) and transferred to arbitrary substrates, such as a centimeter- scale Ti$_3$C$_2$T$_x$ film deposited onto Si/SiO$_2$ (Figure 3b). The light optical contrast of the MXenes on the SiO$_2$ shows that the assembled film consists of a few layers and is only nanometers thick. Planar assembly will not proceed without aging and the inclusion of ligands (Figure S6). The nanosurfactant assembly presents a potential route for the fabrication of large-area MXene films on arbitrary substrates.

The interfacial jamming of MXene nanosurfactants can be leveraged for the formation of structured liquids with arbitrary geometries. In the scenario outlined above, the nanosheet surfactants populate the oil−water interface, saturating the interfacial area. If some external perturbation is applied, for
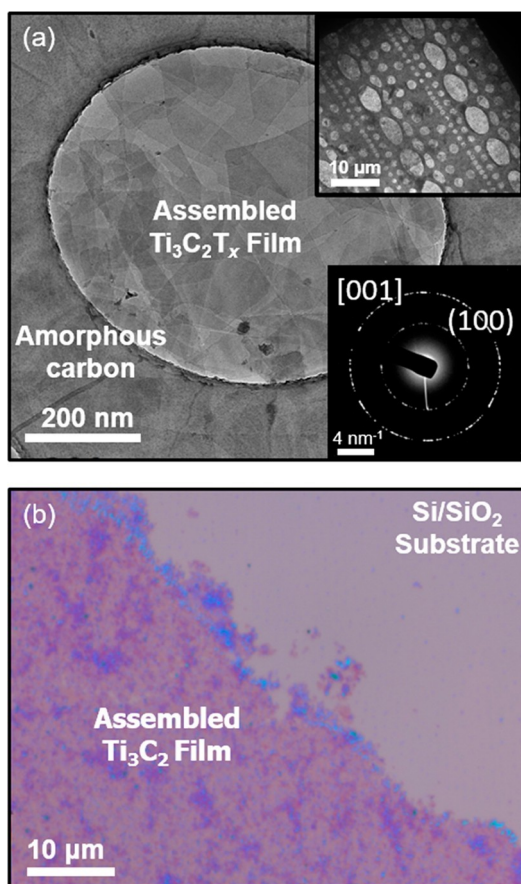
Figure 3. (a) Transmission electron microscopy images of Ti$_3$C$_2$T$_x$ self-assembled at the oil−water interface. Top inset: Low- magnification image showing large-area coverage of the assembled film. Bottom inset: Polycrystalline electron diffraction pattern of the assembled film. (b) Optical images of the self-assembled film that has been transferred to silicon/silicon dioxide wafer.

example an electric field or mechanical force, the surface area may increase, allowing additional MXene nanosheet surfactants to form at the new interface. Once the external perturbation is removed, the interface attempts to relax to its energetic minimum (i.e., minimize surface area); this relaxation is impeded by the jamming of MXene surfactants in the interface, and mechanically metastable geometries are stabilized.

Here, we use this phenomenon to 3D-print liquids in liquids, stabilized by self-assembled MXene surfactants. This is illustrated schematically in Figure 4a. A commercially available 3D printer is modified to extrude the MXene ink at controlled
flow rates, into a high-viscosity silicone oil−ligand matrix. The ink was flowed from standard syringe needles with flow

in water are separated from the silicone oil matrix by the interfacial assembly of MXene sheet surfactants. The size of the printed threads can be tuned by varying the printing parameters, such as print head size, print head speed, and flow rate. This is shown in Figure 4d; at a flow rate of 0.9 mL
min^{-1} the resulting thread has a diameter of approximately 375
μm; this is further increased to 450 and 575 μm for flows of
0.12 and 0.15 mL min^{-1}, respectively.

The 3D printing process is shown in the sequence of images in Figure 4e−g, displaying the 3D nature of the printed constructs. A video of the printing process is available in the Supporting Information. The printed threads are stable over the course of hours to days before individual threads collapse;
however, the printed structures will naturally sink in the oil matrix at a time scale defined by the viscosity of the oil matrix (for high-viscosity silicone oil, sinking occurs in approximately
1 h, Figure S7). The lifespan of the printed threads is determined, in part, by the diameter of the thread, an effect that arises from the variation in the rate of mass transfer across the interface with varying radii of curvature.[33] Depending on thread size, they can persist on time scales ranging from several hours to days. Further, no obvious degradation of the MXenes is observed on that time scale. The 3D printing of liquids in liquids could enable active, adaptive, and reconfigurable constructs. Combined with the high electrical conductivity of MXenes, this provides potential applications for 3D-printed all- liquid reconfigurable electronics, on-demand all-liquid electro-chemical cells, and electrically active, all-liquid fluidic devices.

CONCLUSIONS

In summary, we have demonstrated the formation of MXene nanosheet surfactants at oil−water interfaces. This is accomplished via the interaction of amine-terminated ligands (n-butylamine) with the inherent surface functionalization and negative charge present on Ti$_3$C$_2$T$_x$ sheets. This interaction locks the MXene sheets to the oil−water interface, lowering the interfacial surface tension. It is demonstrated that the
formation of jammed assemblies of the MXene surfactants can be leveraged for the fabrication of planar MXene films and 3D printed all-liquid constructs. These all-liquid MXene assem- blies have potential applications in creating on demand all- liquid electronic, electromagnetic, and electrochemical devices.

EXPERIMENTAL SECTION

MXene Synthesis. Titanium carbide (Ti$_3$C$_2$) MXene was synthesized following a procedure outlined previously.[16] The etchant solution was prepared by adding 3.2 g of lithium fluoride (LiF, Alfa Aesar, −325 mesh powder, 98.5%) to 40 mL of 9 M HCl (Fisher Scientific, 37% solution in water). Then, 2 g of Ti$_3$AlC$_2$ MAX phase (Carbon Ukraine) was added to

the etchant solution over the course 32x centrifugation rates varying from 0.03 to 0.15 mL min^{-1}. Simultaneously, the print head is moved through the oil matrix at speeds of approximately 1000 mm min^{-1}. As the MXene ink is extruded,
the oil−water interface is populated with
MXene surfactants,
forming a jammed assembly stabilizing the printed thread
(inset, Figure 4a) into the path traced by the print head.

The freedom in print geometry is demonstrated by the script "Cal" in Figure 4b. It should be noted that if either the Ti$_3$C$_2$T$_x$ sheets or the ligand is not present, the MXene surfactants do not form and the threads fail to stabilize. This results in a series of drops left in the needle's wake (Figures S4 and S5). In Figure 4c, the details of printing can be seen: tubes of Ti$_3$C$_2$T$_x$

of 5 min. The reaction was stirred at 400 rpm for 24 h at 35 °C. The
etchant solution was washed to pH ~6 with repeated

(100 mL of DI water, 3500 rpm, 5 min) until a dilute green supernatant and swelling of the sediment were observed. Then, 100 mL of DI water was added to the sediment and manually agitated by hand shaking the centrifuge tube for 15 min. The solution was centrifuged for 1 h at 3500 rpm, and the supernatant was decanted. The sediment was dispersed with 50 mL of DI water and centrifuged at 5000 rpm for 10 min. The supernatant after this centrifugation step was purged with argon for 30 min, stored in an argon-sealed headspace vial, and used as the MXene ink to perform interfacial assembly. Concentration of the MXene ink was confirmed by vacuum filtering 5 mL of solution over a polypropylene membrane (Celgard, pore size 0.064 μm) and weighing the mass of the free-standing film
after desiccator drying at ambient temperature. UV−vis spectroscopy
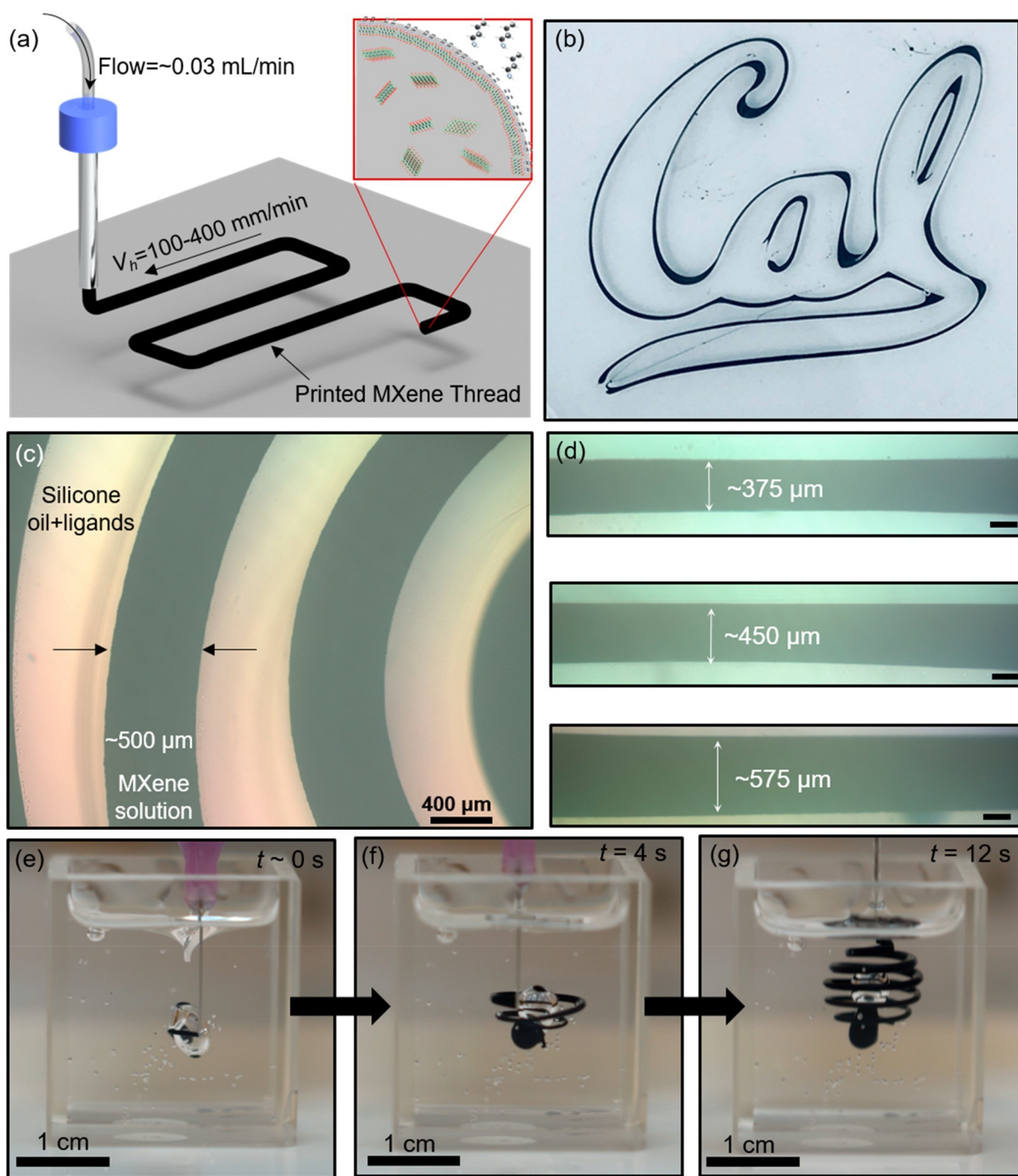
Figure 4. (a) Schematic of the all-liquid 3D printing of $Ti_3C_2T_x$ MXene-stabilized interfacial assemblies in silicone oil. Inset: Schematic of interfacial assembly of MXene sheets plus ligand. (b) Optical image of 3D printed "Cal" logo (field of view ~5 × 5 cm), credit: University of California. (c) Optical images of 3D-printed spiral. (d) Optical images of threads printed with different ink flow rates demonstrating size tunability of printed features; top: $f = 0.09$ mL min^{-1}, middle: $f = 0.12$ mL min^{-1}, and bottom: $f = 0.15$ mL min^{-1}. (e−g) Time sequence of printed three-dimensional assembly. All printing in this figure was carried out with [MXene] = 7.5 mg mL^{-1} and [ligand] = 5 wt % in silicone oil.

(Evolution 201, ThermoScientific) was performed from 200 to 1000 nm in a 10 mm path length quartz cuvette. The Beer−Lambert law and the extinction coefficient of $Ti_3C_2T_x$ (32.44 L g^{-1} cm^{-1} for the LiF/HCl method)[38] were used to verify gravimetric concentration measurements using the extinction measured at the λ_{max} position (~750 nm). Dynamic light scattering (Zetasizer, Nano ZS, Malvern Panalytical) was performed in a polystyrene cuvette. Five measurements were conducted, and the average intensity distribution is reported.

Ink and Matrix Preparation. Dilute dispersions of $Ti_3C_2T_x$ were prepared by mixing DI water with the as-prepared dispersions to the desired concentrations. Dilute dispersions were prepared as-needed and not stored for long periods of time ($t < 3$ h) to avoid potential degradation from dissolved oxygen in the DI water. The pH of diluted dispersions was slightly acidic (~6). TEM imaging of the sheets was conducted using a JEOL 2010 microscope (80 kV). For imaging of individual sheets, dilute solutions were drop cast

onto holey-carbon TEM grids. For the assembled film, films were prepared at a planar interface and scooped out onto holey-carbon grids. High-viscosity

silicone oil (60 000 cSt) and *n*-butylamine were purchased from Sigma-Aldrich. Oil−ligand solutions were prepared by simple dissolution of the ligand into either toluene or high-viscosity silicone oil, depending on the experiment, with concentrations of 1−5 wt %. For mixing of ligands into high-viscosity silicone oil, the ligand−oil mixture was heated to 70 °C in a sealed vial and inverted intermittently over the course of 12 h to encourage thorough mixing. 3D Printing. 3D-printed MXene threads were produced using a commercially available 3D printer (FlashForge Creator Pro), wherein the print head was replaced by a stainless-steel needle (gauge 30, 25, or 14) attached to a syringe pump. GCode for print head trajectories was generated using a python script with commands relayed to the 3D printer using ReplicatorG. Depending on the desired feature sizes, the print head velocity was 0.1−4 mm min^{-1} and the MXene dispersion was injected at a flow rate of 0.01−0.5 mL min^{-1}.

Pendant Drop Tensiometer Measurements. Dynamic inter-facial tension measurements and pendant drop imaging were performed using a Krüss DSA25 drop shape analyzer, with surface tension calculated using the DSA Advance Software. Measurements were obtained by fitting the profile of a pendant drop of MXene dispersion, immersed in toluene that contained the ligands, to the Young−Laplace equation.

Pendant drop tensiometer image of MXene against toluene without ligands, control groups for 3D printing (*i.e.*, printing without MXenes and printing without ligands), and attempt at planar assembly without ligands; further characterization of the starting MXene sheets (PDF)

Video of the printing process (MP4)

AUTHOR INFORMATION

Corresponding Author
*E-mail: azettl@berkeley.edu.

ORCID
Jeffrey D. Cain: 0000-0001-9244-4271
Kathleen Maleski: 0000-0003-4032-7385 Babak Anasori: 0000-0002-1955-253X Yury Gogotsi: 0000-0001-9423-4032 Brett A. Helms: 0000-0003-3925-4174

Notes
The authors declare no competing financial interest.

REFERENCES

(1) Anasori, B.; Gogotsi, Y., Eds. *2D Metal Carbides and Nitrides (MXenes): Structure, Properties and Applications*; Springer: Basel, 2019.

(2) Barsoum, M. W. The $M_{N+1}A_XN$ Phases: A New Class of Solids: Thermodynamically Stable Nanolaminates. *Prog. Solid State Chem.* 2000, *28*, 201−281.

(3) Riedel, R.; Chen, I.-W. *Ceramics Science and Technology*; Wiley-VCH: Weinheim, 2013.

(4) Naguib, M.; Mashtalir, O.; Carle, J.; Presser, V.; Lu, J.; Hultman, L.; Gogotsi, Y.; Barsoum, M. W. Two-Dimensional Transition Metal Carbides. *ACS Nano* 2012, *6*, 1322−1331.

(5) Naguib, M.; Mochalin, V. N.; Barsoum, M. W.; Gogotsi, Y. 25th Anniversary Article: MXenes: A New Family of Two-Dimensional Materials. *Adv. Mater.* 2014, *26*, 992−1005.

(6) Naguib, M.; Kurtoglu, M.; Presser, V.; Lu, J.; Niu, J.; Heon, M.; Hultman, L.; Gogotsi, Y.; Barsoum, M. W. Two-Dimensional Nanocrystals Produced by Exfoliation of Ti_3AlC_2. *Adv. Mater.* 2011, *23*, 4248−4253.

(7) Hart, J. L.; Hantanasirisakul, K.; Lang, A. C.; Anasori, B.; Pinto, D.; Pivak, Y.; van Omme, J. T.; May, S. J.; Gogotsi, Y.; Taheri, M. L. Control of MXenes' Electronic Properties through Termination and Intercalation. *Nat. Commun.* 2019, *10*, 522.

(8) Shahzad, A.; Rasool, K.; Miran, W.; Nawaz, M.; Jang, J.; Mahmoud, K. A.; Lee, D. S. Two-Dimensional $Ti_3C_2T_x$ MXene Nanosheets for Efficient Copper Removal from Water. *ACS Sustainable Chem. Eng.* 2017, *5*, 11481−11488.

(9) Akuzum, B.; Maleski, K.; Anasori, B.; Lelyukh, P.; Alvarez, N. J.; Kumbur, E. C.; Gogotsi, Y. Rheological Characteristics of 2D Titanium Carbide (MXene) Dispersions: A Guide for Processing MXenes. *ACS Nano* 2018, *12*, 2685−2694.

(10) Maleski, K.; Mochalin, V. N.; Gogotsi, Y. Dispersions of Two-Dimensional Titanium Carbide MXene in Organic Solvents. *Chem. Mater.* 2017, *29*, 1632−1640.

(11) Zhang, C.; McKeon, L.; Kremer, M. P.; Park, S.-H.; Ronan, O.; Seral-Ascaso, A.; Barwich, S.; Coileaín, C. O.; McEvoy, N.; Nerl, H. C.; Anasori, B.; Coleman, J. N.; Gogotsi, Y.; Nicolosi, V. Additive-Free MXene Inks and Direct Printing of Micro-Supercapacitors. *Nat. Commun.* 2019, *10*, 1795.

(12) Vural, M.; Pena-Francesch, A.; Bars-Pomes, J.; Jung, H.; Gudapati, H.; Hatter, C. B.; Allen, B. D.; Anasori, B.; Ozbolat, I. T.; Gogotsi, Y.; Demirel, M. C. Inkjet Printing of Self-Assembled 2D Titanium Carbide and Protein Electrodes for Stimuli-Responsive Electromagnetic Shielding. *Adv. Funct. Mater.* 2018, *28*, 1801972.

(13) Hu, G.; Kang, J.; Ng, L. W. T.; Zhu, X.; Howe, R. C. T.; Jones, C. G.; Hersam, M. C.; Hasan, T. Functional Inks and Printing of Two-Dimensional Materials. *Chem. Soc. Rev.* 2018, *47*, 3265−3300.

(14) Kamyshny, A.; Magdassi, S. Conductive Nanomaterials for 2D and 3D Printed Flexible Electronics. *Chem. Soc. Rev.* 2019, *48*, 1712− 1740.

(15) Liu, Y.; Xiao, H.; Goddard, W. A. Schottky-Barrier-Free Contacts with Two-Dimensional Semiconductors by Surface-Engi- neered MXenes. *J. Am. Chem. Soc.* 2016, *138*, 15853−15856.

(16) Alhabeb, M.; Maleski, K.; Anasori, B.; Lelyukh, P.; Clark, L.; Sin, S.; Gogotsi, Y. Guidelines for Synthesis and Processing of Two- Dimensional Titanium Carbide ($Ti_3C_2T_x$ MXene). *Chem. Mater.* 2017, *29*, 7633−7644.

(17) Liu, R.; Li, W. High-Thermal-Stability and High-Thermal- Conductivity $Ti_3C_2T_x$ MXene/Poly(Vinyl Alcohol) (PVA) Compo- sites. *ACS Omega* 2018, *3*, 2609−2617.

(18) Anasori, B.; Lukatskaya, M. R.; Gogotsi, Y. 2D Metal Carbides and Nitrides (MXenes) for Energy Storage. *Nat. Rev. Mater.* 2017, *2*, 16098.

(19) Liang, X.; Garsuch, R.; Nazar, L. F. Sulfur Cathodes Based on Conductive MXene Nanosheets for High-Performance Lithium-Sulfur Batteries. *Angew. Chem., Int. Ed.* 2015, *54*, 3907−3911.

(20) Xia, Y.; Mathis, S.; Zhao, M.-Q.; Anasori, B.; Dang, A.; Zhou, Z.; Cho, H.; Gogotsi, Y.; Yang, S. Thickness-Independent Capacitance of Vertically Aligned Liquid-Crystalline MXenes. *Nature* 2018, *557*, 409−412.

(21) Ren, C. E.; Hatzell, K. B.; Alhabeb, M.; Ling, Z.; Mahmoud, K. A.; Gogotsi, Y. Charge- and Size-Selective Ion Sieving Through $Ti_3C_2T_x$ MXene Membranes. *J. Phys. Chem. Lett.* 2015, *6*, 4026−4031.

(22) hahzad, F.; Alhabeb, M.; Hatter, C. B.; Anasori, B.; Hong, S. M.; Koo, C. M.; Gogotsi, Y. Electromagnetic Interference Shielding with 2D Transition Metal Carbides (MXenes). *Science* 2016, *353*, 1137−1140.

(23) Sarycheva, A.; Polemi, A.; Liu, Y.; Dandekar, K.; Anasori, B.; Gogotsi, Y. 2D Titanium Carbide (MXene) for Wireless Communi- cation. *Sci. Adv.* 2018, *4*, No. eaau0920.

(24) Wei, P.; Luo, Q.; Edgehouse, K. J.; Hemmingsen, C. M.; Rodier, B. J.; Pentzer, E. B. 2D Particles at Fluid−Fluid Interfaces: Assembly and Templating of Hybrid Structures for Advanced Applications. *ACS Appl. Mater. Interfaces* 2018, *10*, 21765−21781.

(25) Kim, F.; Cote, L. J.; Huang, J. Graphene Oxide: Surface Activity and Two-Dimensional Assembly. *Adv. Mater.* 2010, *22*, 1954−1958.

(26) Bian, R.; Lin, R.; Wang, G.; Lu, G.; Zhi, W.; Xiang, S.; Wang, T.; Clegg, P. S.; Cai, D.; Huang, W. 3D Assembly of Ti_3C_2-MXene Directed by Water/Oil Interfaces. *Nanoscale* 2018, *10*, 3621−3625.

(27) Rodier, B.; de Leon, A.; Hemmingsen, C.; Pentzer, E. Controlling Oil-in-Oil Pickering-Type Emulsions Using 2D Materials as Surfactant. *ACS Macro Lett.* 2017, *6*, 1201−1206.

(28) Sun, Z.; Feng, T.; Russell, T. P. Assembly of Graphene Oxide at Water/Oil Interfaces: Tessellated Nanotiles. *Langmuir* 2013, *29*, 13407−13413.

(29) Feng, T.; Hoagland, D. A.; Russell, T. P. Assembly of Acid-Functionalized Single-Walled Carbon Nanotubes at Oil/Water Interfaces. *Langmuir* 2014, *30*, 1072−1079.

(30) Duan, H.; Wang, D.; Kurth, D. G.; Möhwald, H. Directing Self-Assembly of Nanoparticles at Water/Oil Interfaces. *Angew. Chem., Int. Ed.* 2004, *43*, 5639−5642.

(31) Shi, S.; Liu, X.; Li, Y.; Wu, X.; Wang, D.; Forth, J.; Russell, T. P. Liquid Letters. *Adv. Mater.* 2018, *30*, 1705800.

(32) Huang, C.; Forth, J.; Wang, W.; Hong, K.; Smith, G. S.; Helms, B. A.; Russell, T. P. Bicontinuous Structured Liquids with Sub- Micrometre Domains Using Nanoparticle Surfactants. *Nat. Nano- technol.* 2017, *12*, 1060−1063.

(33) Forth, J.; Liu, X.; Hasnain, J.; Toor, A.; Miszta, K.; Shi, S.; Geissler, P. L.; Emrick, T.; Helms, B. A.; Russell, T. P. Reconfigurable Printed Liquids. *Adv. Mater.* 2018, *30*, 1707603.

(34) Feng, W.; Chai, Y.; Forth, J.; Ashby, P. D.; Russell, T. P.; Helms, B. A. Harnessing Liquid-in-Liquid Printing and Micro- patterned Substrates to Fabricate 3-Dimensional All-Liquid Fluidic Devices. *Nat. Commun.* 2019, *10*, 1095.

(35) Schramm, L. L.; Hepler, L. G. Surface and Interfacial Tensions of Aqueous Dispersions of Charged Colloidal (Clay) Particles. *Can. J. Chem.* 1994, *72*, 1915−1920.

(36) Dong, Y.; Chertopalov, S.; Maleski, K.; Anasori, B.; Hu, L.; Bhattacharya, S.; Rao, A. M.; Gogotsi, Y.; Mochalin, V. N.; Podila, R. Saturable Absorption in 2D Ti_3C_2 MXene Thin Films for Passive Photonic Diodes. *Adv. Mater.* 2018, *30*, 1705714.

(37) Mojtabavi, M.; VahidMohammadi, A.; Liang, W.; Beidaghi, M.; Wanunu, M. Single-Molecule Sensing Using Nanopores in Two-Dimensional Transition Metal Carbide (MXene) Membranes. *ACS Nano* 2019, *13*, 3042−3053.

(38) Lipatov, A.; Alhabeb, M.; Lukatskaya, M. R.; Boson, A.; Gogotsi, Y.; Sinitskii, A. Effect of Synthesis on Quality, Electronic Properties and Environmental Stability of Individual Monolayer Ti_3C_2 MXene Flakes. *Adv. Electron. Mater.* 2016, *2*, 1600255.